High-Resolution Geoid Computation by Combining Shipborne and Multi-Satellite Altimetry Data in the Eastern Mediterranean Sea

G.S. Vergos[1], F.A. Bayoud[1] and M.G. Sideris[1] and I.N. Tziavos[2]

[1]Department of Geomatics engineering, University of Calgary, 2500 University Drive N.W., Calgary, Alberta, Canada, T2N 1N4
[2]Department of Geodesy and Surveying, Aristotle University of Thessaloniki, Thessaloniki, Greece

ABSTRACT

The eastern part of the Mediterranean sea, where many geoid solutions exist, is very interesting from the geophysical and geodynamic points of view since it is the place where the Eurasian plate overthrusts the subducting African one. In this study, a new high-resolution multi-satellite (GEOSAT-GM, ERS1-GM, T/P) altimetric geoid is computed and validated, and then combined with shipborne gravity data to obtain the final model. For the low frequency part of the gravity spectrum, we used and compared the results of two geopotential models, EGM96 and GPM98b, complete to degree and order 360 and 1800, respectively. The solutions are compared with T/P data as control points, and with the existing GEOMED solution. We focus on the use of the Multiple Input Multiple Output System Theory (MIMOST) method for the efficient and optimal combination of the heterogeneous data, in which special emphasis is paid to the prediction error estimates. This study is part of a general one aiming at the computation of a high-resolution, high-accuracy geoid for the entire region using altimetry, marine, and land gravity data.

KEYWORDS

Geoid determination, marine geoid, satellite altimetry, sea surface heights, shipborne gravimetry, combination, MIMOST.

1. INTRODUCTION

The Mediterranean Sea has been the spotlight of many geoid computations in the recent years due to its geophysical and geodynamical characteristics. With the advent of altimetry, it became a natural laboratory for geoid and Sea Surface Topography (SST) determinations. In the past ten years, many studies have been conducted, aiming to determine a high-accuracy and high-resolution geoid. Among the many studies, we mention the GEOMED Project, Arabelos and Tziavos (1996), Tziavos et al. (1998), Andritsanos et al. (2000b), Vergos (2000), among others. Our study is focused on the Eastern part of the Mediterranean Sea ($31.5^o \leq \varphi \leq 36.5^o$ and $27.5^o \leq \lambda \leq 35.5^o$) close to the island of Cyprus and the Middle East coastline. Recent analysis of geodetic data, collected in the past two decades, indicate that the eastern part of the Mediterranean Sea has one of the region's largest horizontal motions with respect to a stable Europe (Smith et al., 1994; Le Pichon et al., 1995).

The marine gravity data for the area under study are characterised by their insufficient accuracy. This study aims, using a remove-restore method, at the determination of a high-accuracy and high-resolution geoid by combining all available data sources. Furthermore, we want to investigate whether the combined use of satellite altimetry and shipborne gravity data will improve the geoid modelling compared to the gravimetric geoid only.

Altimetric Sea Surface Heights (SSHs) from the GEOSAT and ERS1 Geodetic Missions (GMs) are used for the computation of the altimetric geoid solution. The land and marine free air gravity anomalies used in this study come from the Bureau Gravimétrique International (BGI, 2000) database.

The gravimetric geoid was computed by the 1D-FFT Stokes convolution (Haagmans et al., 1993; Sideris and She, 1995) using the available free-air gravity anomalies. Shipborne gravity and altimetry data are used for determining a high-resolution ($5' \times 5'$) and high accuracy geoid by optimally combining them with the Multiple Input Multiple Output System Theory (Bendat and Piersol, 1986; Sideris, 1996; Andritsanos et al., 2000a). The above three solutions were referenced to two geopotential models, namely EGM96 (Lemoine et al., 1996), complete to degree and order 360, and GPM98 (Wenzel, 1998), complete to degree and order 1800. As control points and for the validation of our solutions TOPEX/POSEIDON (T/P) SSHs from the 3rd year of the satellite's mission were used. The 3rd year of the T/P mission was selected so that a common observation period between satellites (T/P and ERS1) would be available.

2. ALTIMETRIC GEOID

With the advent of space geodesy and especially during the last fifteen years, satellite altimetry provided the first extensive, long-term and accurate measurement of the Earth's oceans. Satellite altimetry proved to be an accurate and economical, compared to shipborne gravimetry, method to model the oceans and determine the gravity field over large water areas. The geodetic missions of GEOSAT and ERS1 altimetric satellites provide a vast amount of data with resolutions of 2-4km at the equator (Smith et al., 1994). These data cover the Earth's oceans densely and offer precise information due to the accurate models used for the geophysical and instrumental corrections and the modeling of the satellite orbit. Thus, it is possible to compute a marine geoid with an accuracy close to a few centimeters. The altimetric data sets used in this study were GEOSAT-GM newly realized SSHs referred to JGM-3 (Joint Gravity Model 3) orbits provided by NOAA (1997). The observation period of this data set was from March 30th, 1985 to September 30th, 1986. Additional altimetric data were those of the mapping phase of ERS1-GM SSHs from AVISO (1998). The observation period of these altimetric data extends from April 10th, 1994 to March 21st, 1995. Finally, the 3rd year of T/P SSHs distributed by AVISO (1998) were used. The period of observation of this last data set was from October 16th, 1994 to October 8th, 1995. Due to the limited test area the validation tests were first carried out in a larger area ($30^o \leq \varphi \leq 48^o$ and $0^o \leq \lambda \leq 40^o$) in order to compute representative outcomes.

2.1 VALIDATION OF GEOSAT-GM DATA AND GEOID SOLUTION

The GEOSAT-GM SSHs were provided to us in the usual Geophysical Data Record (GDR) format, so a first preprocessing step to correct the SSHs due to the geophysical and instrumental errors, was needed. The models and methods used for the aforementioned corrections are the same as those described in the GEOSAT-GM handbook (1997). In the present study, the signal of the quasi-stationary part of the Dynamic Ocean Topography (DOT) was not taken into account due to the lack of external information about it. Thus, we assumed that the corrected SSHs (174546 point values) can be considered as geoid heights (N). GEOSAT-GM data cover not only sea but some continental areas as well, hence the first test had to deal with the removal of these data. It is well-known that satellite altimetry SSHs give some erroneous values close to the coastline due to the scattering of the radar altimeter pulse from the shallow sea bottom; for that reason, data close to the coastline were removed, as well. A $1' \times 1'$ bathymetric model for the Mediterranean Sea was used (Sandwell, 1996) and an interpolation of depth values was carried out at the points where SSHs from GEOSAT-GM were available. Then, data points with depths

greater than –200m were neglected (see Table 1). According to this test, 25855 point values (14.82%) were finally removed (see Table 1).

max	min	mean	std
240.151	-286.336	29.553	±13.323
240.151	-286.336	28.858	±13.428

Table 1. GEOSAT-GM data before and after the bathymetry test. Unit: [m].

From Table 1, even after the bathymetry test, some extreme minimum and maximum values are still evident, thus indicating the presence of outliers. After the bathymetry test the long wavelength part of the geoid heights was removed by subtracting the contribution of EGM96 (Lemoine et al., 1996) and GPM98b (Wenzel, 1998) geopotential models from the SSHs. The statistics of the so derived residual geoid heights (N_{res}) are summarized in Table 2.

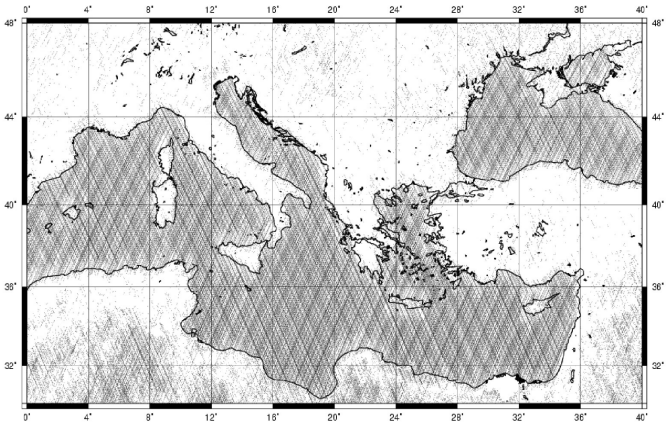

(a)

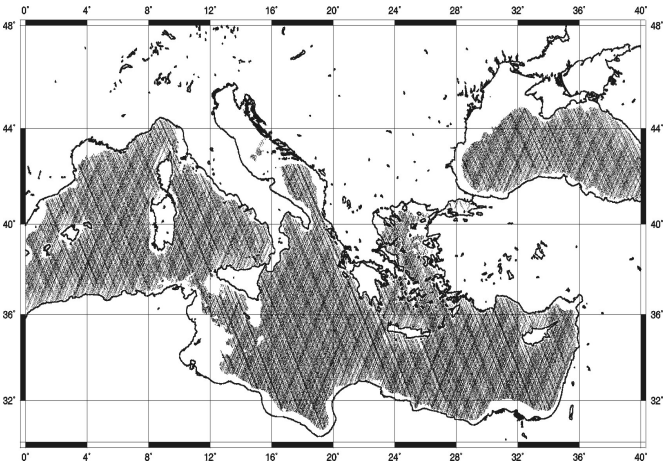

(b)

Figure 1. GEOSAT-GM data distribution before (a) and after (b) the bathymetry test.

	max	min	mean	std
$\mathbf{N_{res}}$ (EGM96)	212.341	-324.884	-0.473	±2.737
$\mathbf{N_{res}}$ (GPM98b)	212.823	-324.557	-0.502	±2.648

Table 2. GEOSAT-GM residual undulations. Unit: [m]

The residual geoid heights in Table 2 indicate a number of unexpected values. This is due to the presence of blunders and/or systematic errors. In order to remove these large values, an additional 3rms test for blunder detection was performed for the entire Mediterranean Sea. This resulted in the removal of 1926 residual geoid heights (1.3%) in the case of EGM96 and 1379 residual geoid heights (0.93%) in the case of GPM98b. To summarize, during the two validation tests (bathymetry and 3rms) 27781 GEOSAT-GM geoid heights (15.9%) reduced to EGM96 geopotential model and 27324 geoid heights (15.6%) reduced to GPM98b were eliminated. The remaining residual geoid heights in the area under study ($30^o \leq \varphi \leq 38^o$ and $27^o \leq \lambda \leq 36^o$) are 24563 and 24621 referenced to EGM96 and GPM98b fields, respectively. The statistics of these residual geoid heights in the test area are given in Table 3.

	max	min	mean	std
$\mathbf{N_{res}}$ (EGM96)	1.482	-1.490	-0.337	±0.321
$\mathbf{N_{res}}$ (GPM98b)	1.527	-1.816	-0.764	±0.265

Table 3. GEOSAT-GM residual undulations in the area under study, after the 3rms test. Unit: [m]

Comparing Tables 2 and 3, a refinement of the GEOSAT residual geoid heights in terms of minimum, maximum and standard deviation values is obvious. To these residual geoid heights, a bias and tilt crossover adjustment was applied for the minimization of the orbital errors. Comparing the residual geoid heights before and after the adjustment, insignificant improvement, for the case of EGM96, and slight deterioration, for the case of GPM98, in terms of the standard deviation and the mean value of the differences were detected. This can be mainly attributed to the improved and high accuracy orbits used for the present release of the GEOSAT-GM GDRs (JGM3). We believe that this is a good indication that the remaining radial orbit errors in the GEOSAT-GM data are very small and a crossover adjustment is not needed to reduce it. On the other hand, crossover adjustment can be very useful in reducing the influence of oceanic phenomena contaminating geodetic mission data, especially in regions with high sea surface variability (SSV) located in purely oceanic regions and not in a closed sea area like the Mediterranean Sea. For these reasons, the residual geoid heights after the 3rms test and before adjustment were used for the subsequent geoid determination. In the next step the point residual geoid heights were interpolated onto a $5' \times 5'$ grid. Then, as a final step of the GEOSAT-GM data processing, the contribution of EGM96 and GPM98b geopotential models to the residual geoid heights was restored and the final geoid height solutions of GEOSAT-GM altimetry data were calculated (see Table 4).

	max	min	mean	std
N (EGM96)	37.977	0.669	18.263	±8.443
N (GPM98b)	37.873	0.671	18.477	±8.383

Table 4. The final geoid solution from GEOSAT-GM altimetry data. Unit: [m]

2.2 VALIDATION OF ERS1-GM DATA AND GEOID SOLUTION

The preprocessing step for the ERS1-GM SSHs included, as with the case of GEOSAT-GM, the correction of the data due to the geophysical and instrumental errors according to the models and methods described in AVISO handbook (AVISO, 1998). The total number of corrected ERS1-GM SSHs available for the Mediterranean Sea was 105105 point values. Then the contribution of the EGM96 and GPM98b geopotential models was removed from the corrected SSHs. The statistics of the derived residual geoid heights are shown in Table 5.

	max	**min**	**mean**	**std**
$\mathbf{N_{res}}$ (EGM96)	1.572	-2.062	-0.223	±0.347
$\mathbf{N_{res}}$ (GPM98b)	2.832	-1.816	-0.216	±0.467

Table 5. ERS1-GM residual undulations. Unit: [m]

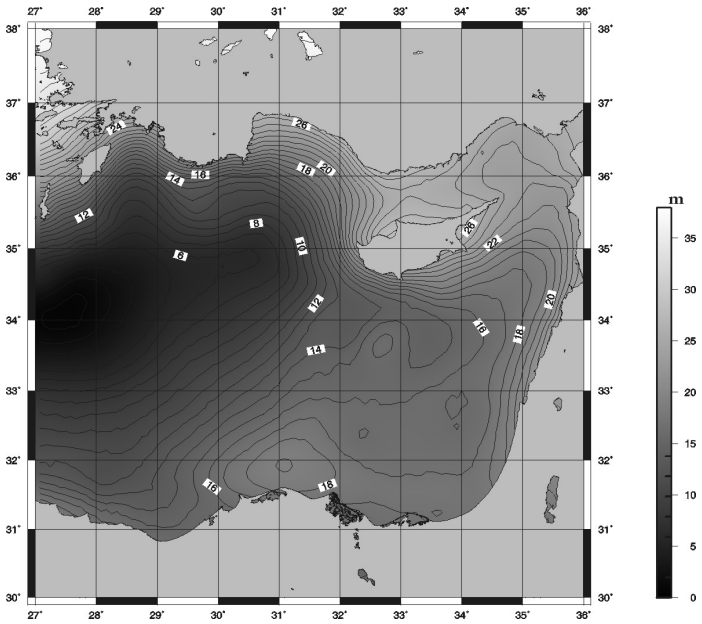

Figure 2. The final geoid solution from GEOSAT-GM to GPM98 reference filed.

In a further step, and in order to detect the presence of blunders, a 3rms test was applied to the residual geoid heights during which 866 (0.0087%) for EGM96 and 35 (0.00033%) point residual geoid heights were removed. The statistical results of this numerical test for the area under study are summarized in Table 6. As in the case of GEOSAT-GM N_{res}, a crossover adjustment was applied with the same results as the ones discussed before.

	max	**min**	**mean**	**std**
$\mathbf{N_{res}}$ (EGM96)	1.098	-1.181	-0.264	±0.315
$\mathbf{N_{res}}$ (GPM98b)	1.014	-1.436	-0.653	±0.253

Table 6. ERS1-GM residual undulations in the area under study, after the 3rms test. Unit: [m]

The data after the 3rms test were then used for the prediction on a 5′×5′ grid. The contribution of the geopotential models was restored in these gridded residual geoid heights. The statistics of the final ERS1-GM geoid height solutions are given in Table 7. The final altimetric geoid solutions are depicted in Figure 3.

	max	**min**	**mean**	**std**
N (EGM96)	37.717	0.669	18.263	±8.443
N (GPM98b)	37.958	0.712	18.594	±8.417

Table 7. The final geoid solution from ERS1-GM altimetry data. Unit: [m]

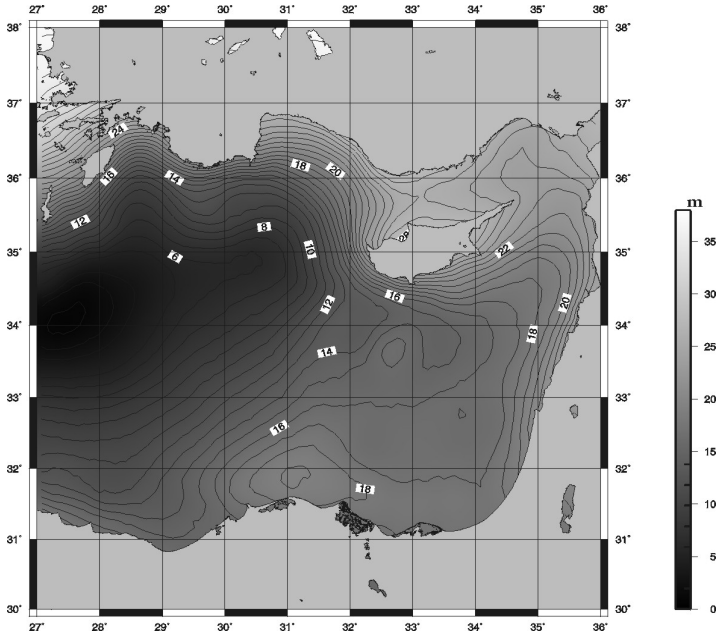

Figure 3. The final geoid solution from ERS1-GM to GPM98 reference field.

3. GRAVIMETRIC GEOID

The gravity data used were sea and land free-air gravity anomalies in the area under study. 18618 marine free-air gravity anomalies and 724 land free-air gravity anomalies, for the island of Cyprus, were used (BGI, 2000). The statistics of this dataset are reported in Table 8 and the data distribution is depicted in Fig. 4.

	max	**min**	**mean**	**std**
Δg	140.000	-239.000	-63.595	±58.105

Table 8. Statistics of gravity data. Unit: [mGal]

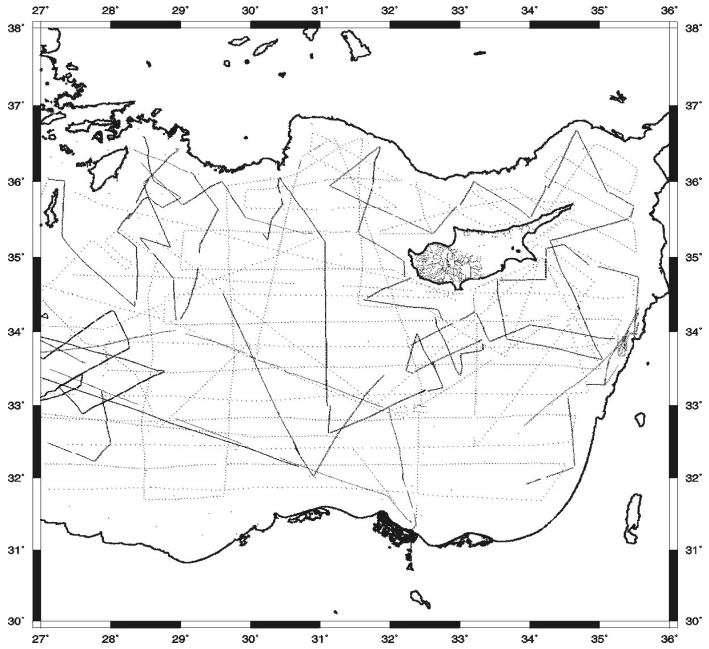

Figure 4. Distribution of gravity data in the area under study.

All these gravity data values were first reduced to EGM96 and GPM98b reference surfaces (Table 9). Then these residual gravity anomalies were gridded on a 5′×5′ grid and the computation of the residual geoid heights was carried out by applying the 1-D FFT spherical Stokes convolution (Haagmans et al., 1993; Sideris and She, 1995):

$$N^{gr} = \frac{R\Delta\varphi\Delta\lambda}{4\pi\gamma}\mathcal{F}_1^{-1}\left\{\sum_{\varphi=\varphi_1}^{\varphi_n}\mathcal{F}_1\{S\}\mathcal{F}_1\{\Delta g\cos\varphi\}\right\} \quad (1)$$

Where N^{gr} is the gravimetric geoid height, R is the mean earth radius, γ is the normal gravity, Δg denotes gravity anomaly, and $S(\psi)$ is Stokes' function. The statistics of these residual geoid heights are reported in Table 10.

	max	**min**	**mean**	**std**
$\mathbf{N_{res}}$ (EGM96)	160.552	-113.760	-8.887	±18.430
$\mathbf{N_{res}}$ (GPM98b)	158.032	-93.616	-8.240	±11.033

Table 9. Statistics of reduced gravity anomalies to EGM96 and GPM98b reference fields. Unit: [mGal]

	max	**min**	**mean**	**std**
$\mathbf{N_{res}}$ (EGM96)	-0.865	-4.001	-2.469	±0.521
$\mathbf{N_{res}}$ (GPM98b)	-0.848	-3.127	-2.210	±0.445

Table 10. Statistics of residual gravimetric geoid undulations. Unit: [m]

The final gravimetric geoid solutions were then calculated by restoring the contribution of the reference models EGM96 and GPM98b to geoid height residuals. The statistics of these solutions are given in Table 11. Finally, we depict the gravimetric geoid height solutions for both reference fields in Figures 5 and 6.

	max	**min**	**mean**	**std**
N (EGM96)	30.196	-0.037	13.484	±6.256
N (GPM98b)	29.654	-0.139	13.220	±6.183

Table 11. The final gravimetric geoid solution to EGM96 and GPM98b reference fields. Unit: [m]

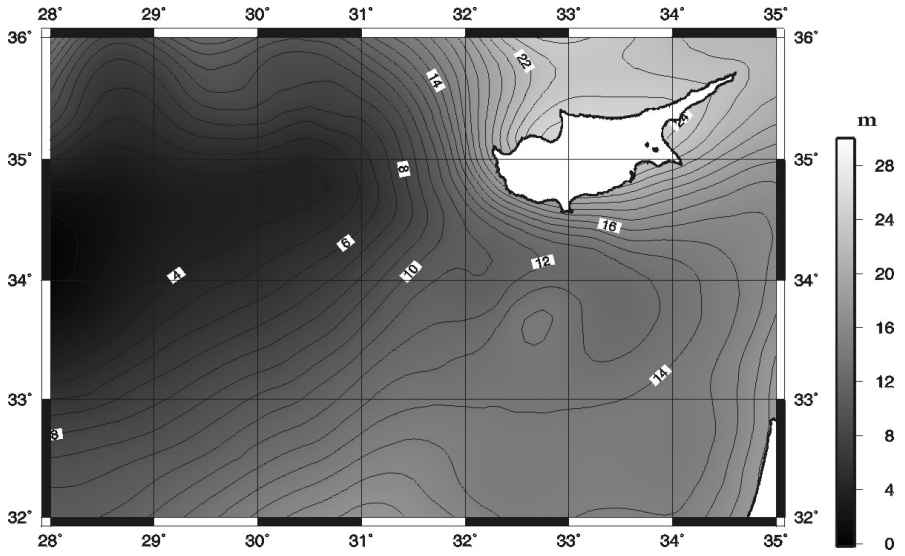

Figure 5. The final gravimetric geoid solution to EGM96 reference field.

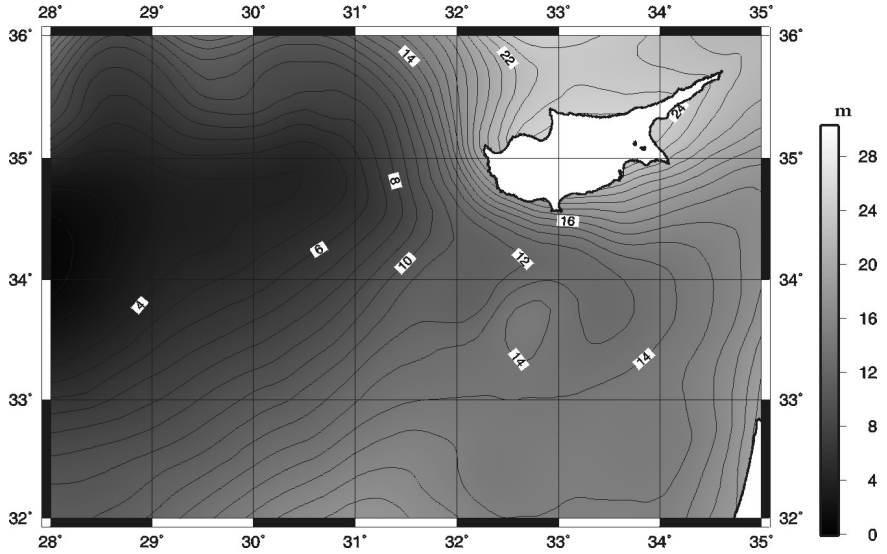

Figure 6. The final gravimetric geoid solution to GPM98 reference field.

4. Combined method and geoid solution

Having determined the altimetric and gravimetric geoid height solutions, combined ones were computed using the Multiple Input Multiple Output System Theory (MIMOST) as presented in Andritsanos et al. (2000a), Andritsanos et al. (2000a). The data used for the combination method are the residual altimetric geoid heights from ERS1-GM and GEOSAT-GM reference to EGM96 and GPM98b fields and the corresponding data from the gravimetric geoid solutions.

Due to the lack of specific information about the errors in both the altimetric and the gravimetric solution, simulated noises were used as input error. Randomly distributed fields (white noise) were generated in MATLAB® using 5cm standard deviation for the altimetry derived geoid heights and 10cm standard deviation for the gravimetric one. The final solution from the combination method, as well as the output error PSD function, were calculated according to the following equations:

$$\hat{N}_o = \begin{bmatrix} H_{\hat{N}N_g} & H_{\hat{N}N_a} \end{bmatrix} \left(\begin{bmatrix} P_{N_{og}N_{og}} & P_{N_{og}N_{oa}} \\ P_{N_{oa}N_{og}} & P_{N_{oa}N_{oa}} \end{bmatrix} - \begin{bmatrix} P_{m_g m_g} & 0 \\ 0 & P_{m_a m_a} \end{bmatrix} \right) \begin{bmatrix} P_{N_{og}N_{og}} & P_{N_{og}N_{oa}} \\ P_{N_{oa}N_{og}} & P_{N_{oa}N_{oa}} \end{bmatrix}^{-1} \begin{bmatrix} N_{og} \\ N_{oa} \end{bmatrix} \tag{2}$$

$$\begin{aligned} P_{\hat{e}\hat{e}} = \Bigg\{ & \begin{bmatrix} H_{\hat{N}N_g} & H_{\hat{N}N_a} \end{bmatrix} \left(\begin{bmatrix} P_{N_{og}N_{og}} & P_{N_{og}N_{oa}} \\ P_{N_{oa}N_{og}} & P_{N_{oa}N_{oa}} \end{bmatrix} - \begin{bmatrix} P_{m_g m_g} & 0 \\ 0 & P_{m_a m_a} \end{bmatrix} \right) - \begin{bmatrix} \hat{H}_{\hat{N}_o N_{og}} & \hat{H}_{\hat{N}_o N_{oa}} \end{bmatrix} \\ & \begin{bmatrix} P_{N_{og}N_{og}} & P_{N_{og}N_{oa}} \\ P_{N_{oa}N_{og}} & P_{N_{oa}N_{oa}} \end{bmatrix} \Bigg\} \left(\begin{bmatrix} H^*_{\hat{N}N_g} \\ H^*_{\hat{N}N_a} \end{bmatrix} - \begin{bmatrix} \hat{H}^*_{\hat{N}_o N_{og}} \\ \hat{H}^*_{\hat{N}_o N_{oa}} \end{bmatrix} \right) + \begin{bmatrix} \hat{H}_{\hat{N}_o N_{og}} & \hat{H}_{\hat{N}_o N_{oa}} \end{bmatrix} \begin{bmatrix} P_{m_g m_g} & 0 \\ 0 & P_{m_a m_a} \end{bmatrix} \begin{bmatrix} H^*_{\hat{N}N_g} \\ H^*_{\hat{N}N_a} \end{bmatrix} \end{aligned} \tag{3}$$

where $\hat{N}_o$ is the spectrum combined geoid solution, N_g and N_a are the spectra of the pure gravimetric and altimetric signals respectively, N_{og} and N_{oa} are the spectra of gravimetric and altimetric observations, m_g and m_a are the input noises, H_{xy} is the theoretical operator that connects the pure input y and output signals x, $\hat{H}_{x_o y_o}$ is the optimum frequency impulse response function, $\hat{e}$ is the output noise and P_{xy} are PSD functions (Andritsanos et al, 2000a). The statistics of the final geoid height solution from the optimal combination of the heterogeneous heights referenced to the EGM96 and GPM98b geopotential models can be seen in Table 12 and are depicted in Figure 7.

	max	**min**	**mean**	**std**
N (EGM96)	32.210	0.613	15.036	±6.461
N (GPM98b)	32.042	1.103	15.301	±6.210

Table 12. The combined geoid solution to EGM96 and GPM98b reference fields. Unit: [m]

5. COMPARISON OF THE COMPUTED GEOID HEIGHT SOLUTIONS WITH T/P SSHS AND GEOMED

The previously described geoid height solutions were compared with stacked T/P SSHs from the 3rd year of the satellite mission, which are considered as geoid heights when neglecting the SST signal. T/P

SSHs are known for their high accuracy and they can be safely used as control points for our solutions. Additionally, we present the comparison between the geoid solution from the combination method and the GEOMED geoid for the Mediterranean Sea. From Table 13 and Figure 8, we can see that the differences with GEOMED are at the ±56cm and ±63cm level when using EGM96 and GPM98b as reference fields for our combined solution. This can be mainly attributed to the different reference fields used (GEOMED uses OSU91A as a reference field) and the more accurate altimetry data used in the present study.

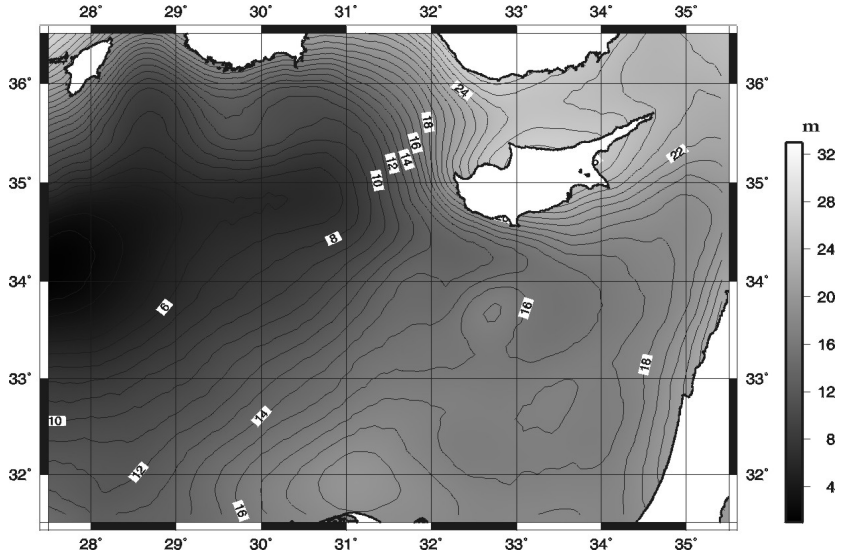

(a)

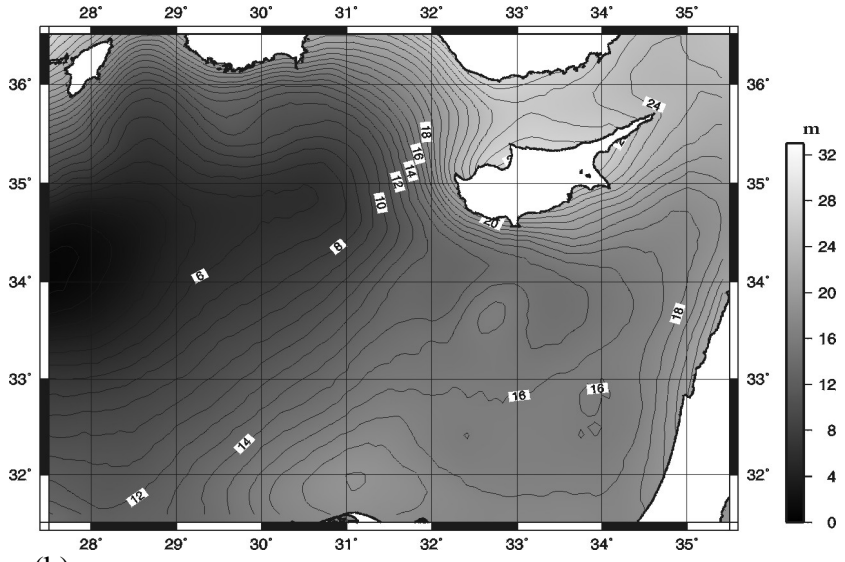

(b)

Figure 7: The final geoid height solutions from the MIMOST method to EGM96 (a) and GPM98b (b) reference surfaces.

N_{dif}	max	min	mean	std
(EGM96)	2.621	-0.778	0.984	±0.559
(GPM98b)	3.370	-0.694	0.625	±0.635

Table 13. Statistics of the differences between GEOMED and the combined solution. Unit: [m]

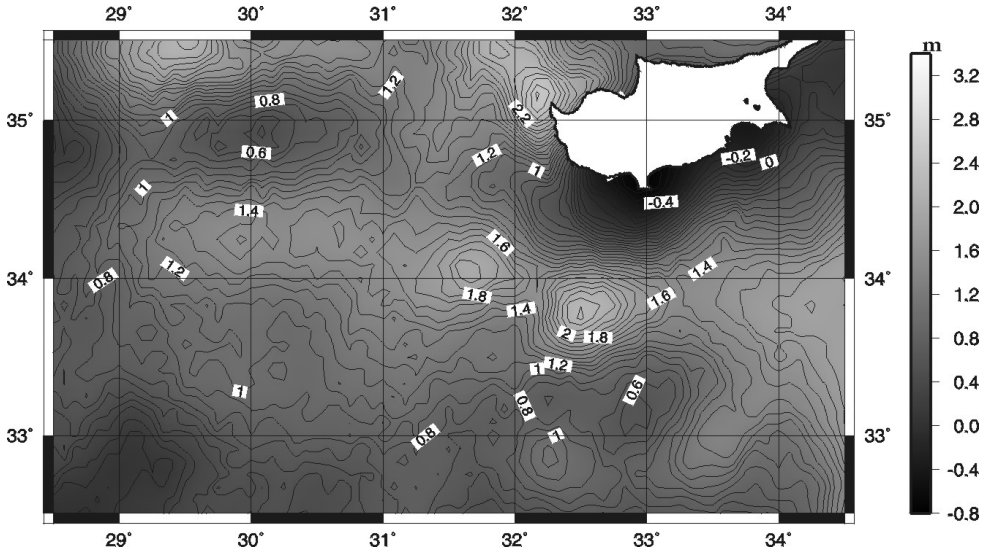

(a)

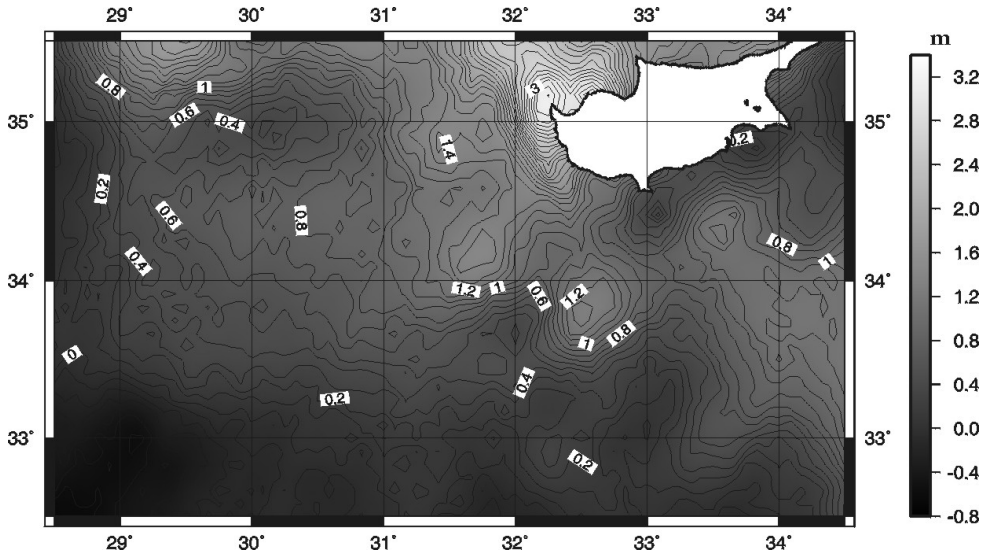

(b)

Figure 8. Geoid height differences between GEOMED and the final combined solutions from the MIMOST method for EGM96 (a) and GPM98b (b) reference surfaces.

For the comparisons between the aforementioned solutions and the stacked SSHs from the 3rd year of the T/P mission the computed differences were minimized by using a four-parameter transformation model:

$$SSH_{T/P} = N - b_o \cos\phi\cos\lambda - b_1 \cos\phi\sin\lambda - b_2 \sin\phi - b_3 \quad (4)$$

where the parameters b_o, b_1, b_2 and b_3 were calculated by the least squares technique and N is the altimetric, gravimetric or combined geoid height depending on the solution under consideration. Comparing the standard deviation of the differences between the different geoid height solutions and the stacked T/P heights, it is easily concluded that the altimetric solutions are superior to the gravimetric ones. When comparing the pure altimetric geoid heights with T/P SSHs, the accuracy is at the level of ±8 for both satellites (see figures 9). The differences for the gravimetric solutions on the other hand reach the level of ±20cm in terms of standard deviation (see figure 10). The comparison between the optimally combined geoid heights and the stacked T/P SSHs reach an accuracy close to ±7cm in terms of standard deviation of the differences for GPM98b but ±29cm for EGM96 (see figure 11).

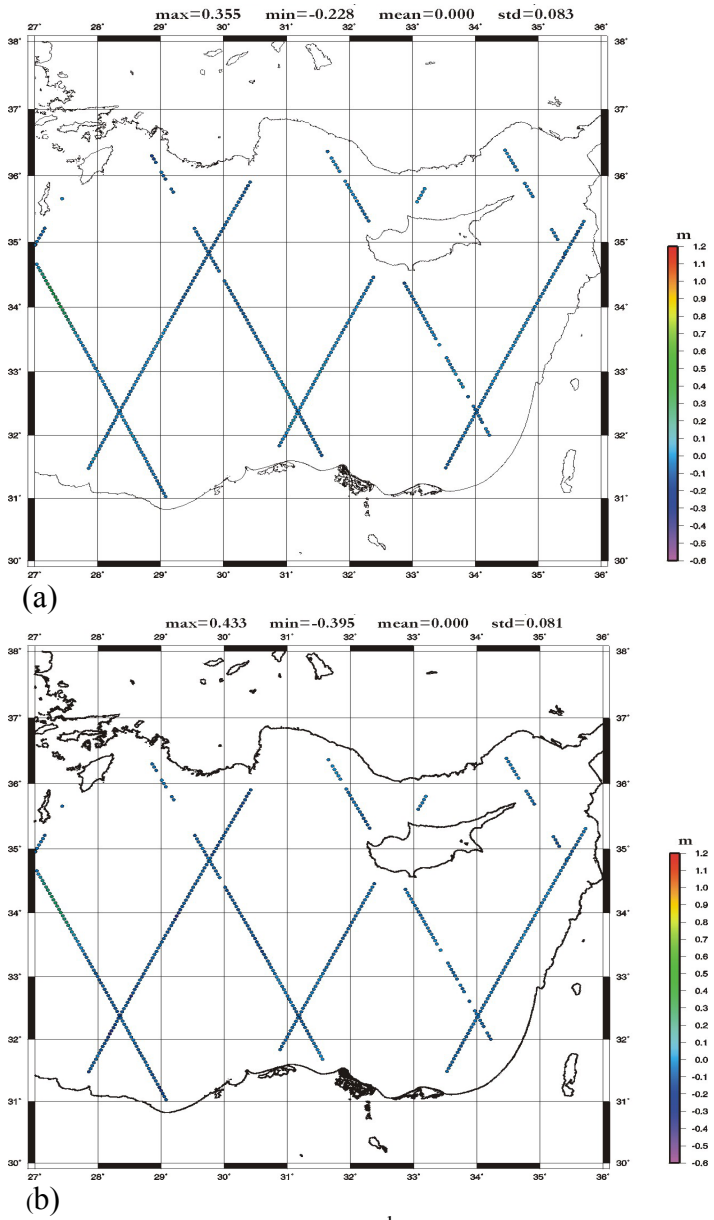

(a)

(b)

Figure 9. Differences between stacked T/P SSHs (3rd year) and ERS1-GM (a) and GEOSAT-GM (b) geoid height solutions (GPM98b reference field). Unit: [m]

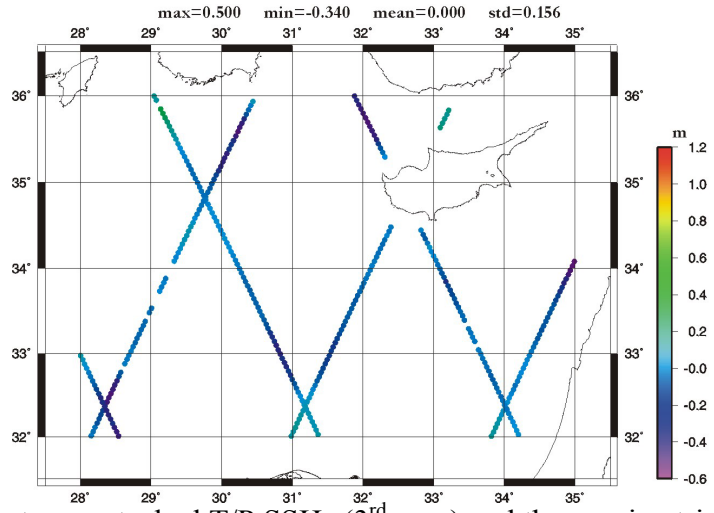

Figure 10. Differences between stacked T/P SSHs (3rd year) and the gravimetric geoid height solution to GPM98b reference field. Unit: [m]

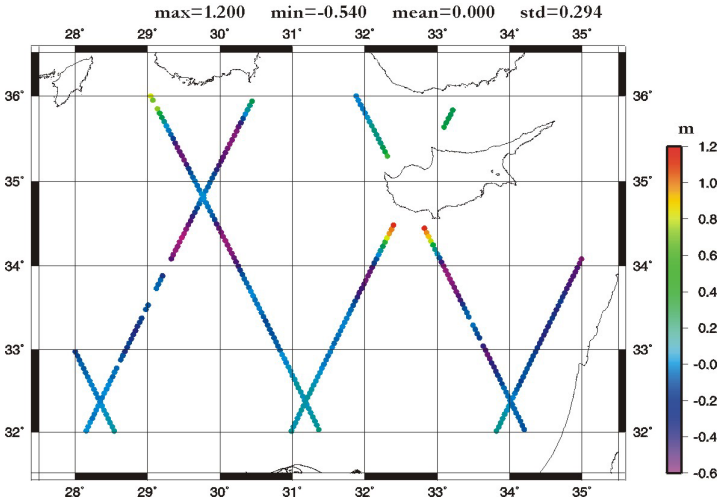

(a)

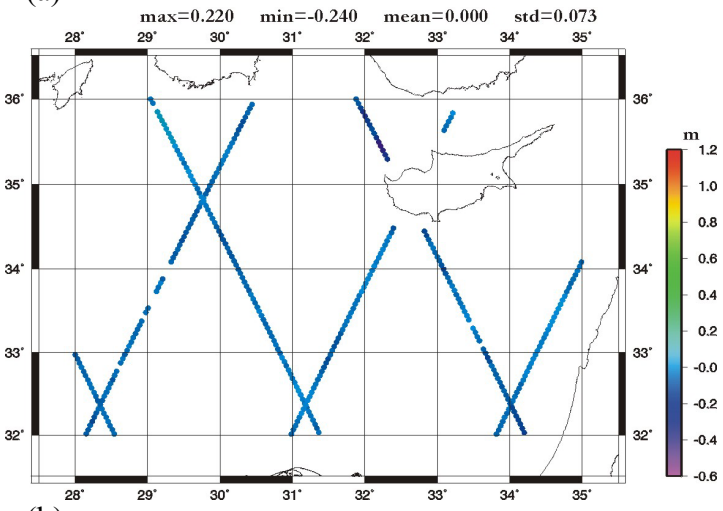

(b)

Figure 11: Differences between stacked T/P SSHs (3rd year) and the final geoid height solutions from the MIMOST method to EGM96 (a) and GPM98b (b) reference models. Unit: [m]

6. CONCLUSIONS – FUTURE PLANS

Eight local geoid solutions were computed for the Eastern part of the Mediterranean Sea close to the island of Cyprus. Satellite altimetry, marine and land gravity data were used in a combined solution for the optimal determination of the geoid in the area under study.

The well-known remove-restore method was used for the altimetric and gravimetric geoid determination when the gravimetric residual geoid heights are determined using the 1-D FFT method. Finally the Multiple Input Multiple Output System Theory was used to optimally combine the available data sets.

Based on these results the determination of a purely altimetric geoid is possible with an accuracy close to ±5cm while the determination of a purely gravimetric one has a lower accuracy close to ±18cm. The differences between T/P SSHs and the gravimetric geoid heights can be mainly attributed to the unavailable SST signal and the poor accuracy of the available gravity data. Nevertheless the achieved accuracy of the gravimetric geoid is better compared to a study by Vergos (2000) for an area northwest of the present one, where the available gravity data came from the digitization of the Morelli's maps (Behrend et al. 1996) and had even lower accuracy.

As far as the combined solution is concerned, it is evident that the use of altimetry data, at least when using GPM98 as a reference field, improve by ±9cm the accuracy of geoid determination as compared to the gravimetric only solution. This can be attributed not only to the use of altimetry data but to the noise level used for the different data sets (5cm for the altimetric and 10cm for the gravimetric ones) which give more weight to the altimetric geoid heights in the combination algorithm. Throughout this research, GPM98b proved to give better agreement, compared to EGM96, with our control datasets. This is an indication that GPM98b is more appropriate, at least for the Mediterranean Sea, to be used as the reference field when geoid modeling is concerned.

A detailed study of the different solutions, with more emphasis on the error spectrum, and an investigation of the frequency contents of the two geopotential models is needed and will be carried out. In order to obtain a higher resolution and higher accuracy geoid solution in the area under study, a significant improvement of both land and sea gravity databases is necessary. It is expected that the forthcoming gravity field dedicated satellite missions will contribute to the improvement of such databases.

Acknowledgements

The financial assistance provided to the first two of the authors by the GEOIDE Network of Centers of Excellence is gratefully acknowledged. We extensively used the Generic Mapping Tools Version 3.1 (Wessel and Smith, 1998) in displaying our results.

References

Andritsanos, V.D., M.G. Sideris and I.N. Tziavos. *A survey of gravity field modelling applications of the Input-Output System Theory (IOST)*. To appear in IGeS Bulletin, 2000a.

Andritsanos, V.D., M.G. Sideris and I.N. Tziavos. *Quasi-stationery Sea Surface topography estimation by the multiple Input-Output method*. Accepted for publication in Journal of Geodesy, 2000b.

AVISO User Handbook – Corrected Sea Surface Heights (CORSSHs). AVI-NT-011-311-CN, Edition 3.1, 1998.

Arabelos, D. and I.N. Tziavos. *Combination of ERS1 and TOPEX altimetry for precise geoid and gravity* recovery. Geophys. J. Int., 125, pp. 285-312, 1996.

Behrend, D., H. Denker, and K. Schmidt. *Digital gravity data sets for the mediterranean sea derived from available maps*. Bulletin d' information, No 78, pp. 31-39, BGI, 1996.

Bendat, J.S. and Piersol A.G. *Random data: Analysis and Measurement Procedures*. Second edition. John Wiley and Sons, New York, 1986.

Bureau Gravimétrique International. *Shipborne gravity data for the Eastern Mediterranean Sea*. Personal communication, 2000.

The Geosat Altimeter JGM-3 GDRs Handbook. Internet Resources:http://www.ibis.gdrl.noss.gov/SAT/gdrs/geosat-handbook, 1997.

GEOMED group. *Mare Nostrum – GEOMED*. Report No. 4, Department of Geodesy and Surveying, Aristotle University of Thessaloniki, Thessaloniki, Greece, 1993. Eds.: D. Arabelos and I.N. Tziavos

Haagmans, R., E. de Min and M. van Gelderen. *Fast evaluation of convolution integrals on the sphere using 1D FFT, and a comparison with existing methods for Stokes' integral*. Manuscr. Geod. 18, pp. 227-241, 1993.

Lemoine, F.G., et al. *The development of the join NASA GSFC and NIMA geopotential model EGM96*, NASA Technical Paper, 1998 – 206861, 1998.

National Oceanographic and Atmospheric Administration - NOAA. *The GEOSAT-GM Altimeter JGM-3 GDRs*. 1997.

Pichon Le, X.J. Angelier, N. Chamot-Rooke, S. Lallemant, R. Noomen, G. Veis. *Geodetic determination of the kinematics of Central Greece with respect to Europe: Implications for Eastern Mediterranean Tectonics*. Journal of Geophysical Research, Vol. 100, 12265-12690, 1995.

Sandwell D. *Data Base Description for Digital Bathymetric Data Base-Variable Resolution (DBDB-V)*. Version 1.0, Naval Oceanographic Office, Stennis Space Center, March, 1996

Sideris, M.G. *On the use of heterogeneous noisy data in spectral gravity field modeling methods*. Journal of Geodesy, 70, pp. 470-479, 1996.

Sideris, M.G. and B.B. She. *A new high-resolution geoid for Canada and part of the U.S. by 1D-FFT method*. Bull. Geod. 69:92-108, 1995.

Smith D.E., R. Kolenkiewicz, J.W. Robbins, P.J. Dunn, M.H. Torrence. Horizontal crustal motion in the Central and Eastern Mediterranean inferred from Satellite Laser Ranging measurements. *Geophysical Research Letter*, 21, 1979 – 1982, 1994b.

Smith, W.H.F. and D.T. Sandwell. *Bathymetric prediction from dense satellite altimetry and sparse shipboard bathymetry*. Journal of Geophysical Research, 99, No. B11, 21803-21824, 1994.

Tziavos, I.N., M.G. Sideris and R. Forsberg. *Combined satellite altimetry and shipborne gravimetry data processing*. Marine Geodesy, 21, pp.299-317, 1998.

Vergos, G.S., *The contribution of satellite altimetry to gravity field modeling – A case of study in the Eastern Mediterranean*. Diploma thesis, School of Rural and Surveying Engineering, Faculty of Engineering, Aristotle University of Thessaloniki, Department of Geodesy and Surveying, 2000.

Wenzel, H.G. *Global models of the gravity field of high and ultra-high resolution*. In Lecture Notes of IAG's Geoid School, Milano, Italy, 1999.

Wessel, P., and W.H.F. Smith. *New improved version of Generic Mapping Tools released*. EOS Trans. Amer. Geophys. U., vol. 79 (47), pp. 579, 1998.

Correspondence to: Georgios S. Vergos, Department of Geomatics Engineering, The University of Calgary, 2500 University Drive N.W., Calgary, Alberta, Canada, T2N 1N4, ++1 (403) 220-4113, **gsvergos@ucalgary.ca**